Porcine deltacoronavirus engages the transmissible gastroenteritis virus functional receptor porcine aminopeptidase N for infectious cellular entry

Bin Wang*, Yan Liu*, Chun-Miao Ji*, Yong-Le Yang, Qi-Zhang Liang, Pengwei Zhao, Ling-Dong Xu, Xi-Mei Lei, Wen-Ting Luo, Pan Qin, Jiyong Zhou, Yao-Wei Huang

Institute of Preventive Veterinary Medicine and Key Laboratory of Animal Virology of Ministry of Agriculture, College of Animal Sciences, Zhejiang University, Hangzhou, Zhejiang 310058, China.

*These authors contributed equally to this work.

Correspondence: Yao-Wei Huang, yhuang@zju.edu.cn Tel: 86-571-88982051

Running title: Porcine APN as PDCoV entry receptor

Word counts: manuscript text (4,152 words); abstract (212 words); importance (150 words).

Figure number: 6

Abstract

Identification of cellular receptors used by coronavirus (CoV) entry into the host cells is critical to understand pathogenesis and to develop intervention strategies. The fourth CoV genus, *Deltacoronavirus*, evolutionally related to the *Gammacoronavirus*, has just been defined recently. In the current study, we demonstrate that porcine aminopeptidase N (pAPN) acts as a cross-genus CoV functional receptor for both enteropathogenic porcine DeltaCoV (PDCoV) and AlphaCoV (transmissible gastroenteritis virus, TGEV) based upon three lines of evidences. First, the soluble S1 protein of PDCoV efficiently bound to surface of target porcine cell lines known to express pAPN as TGEV-S1 did, which could be blocked by soluble pAPN pre-treatment. Second, either PDCoV-S1 or TGEV-S1 physically recognized and interacted with pAPN by co-immunoprecipitation in pAPN-cDNA-transfected cells and by dot blot hybridization assay. Finally, exogenous expression of pAPN in refractory cells conferred susceptibility to PDCoV-S1 binding and for PDCoV entry and productive infection. PDCoV-S1 appeared to have a lower pAPN-binding affinity and likely consequent lower infection efficiency in pAPN-expressing refractory cells as compared to TGEV-S1, suggesting that there may be difference in virus-binding regions in pAPN between these two viruses. This study paves the way for dissecting the molecular mechanisms of PDCoV-host interactions and pathogenesis as well as facilitates future vaccine development and intervention strategies against PDCoV infection.

Keywords: Cellular receptor; Coronavirus; Aminopeptidase N (APN); Porcine deltacoronavirus (PDCoV); Entry

43 **Importance**

44 The emergence of new human and animal coronaviruses is believed to have occurred
45 through interspecies transmission that is mainly mediated by species-specific receptor of the
46 host. Among the four genera of the *Coronavirinae*, a couple functional receptors for the
47 representative members in the genera *Alphacoronavirus* and Betacoronavirus have been
48 identified, whereas receptors for *Gammacoronavirus* and *Deltacoronavirus*, which are
49 believed to originate from birds, are still unknown. Porcine coronaviruses including the
50 newly discovered porcine deltacoronavirus (PDCoV) associated with diarrhea in newborn
51 piglets have posed a serious threat to the pork industry in Asia and North America. Here we
52 report that PDCoV employs alphacoronavirus TGEV functional receptor porcine
53 aminopeptidase N (pAPN) for cellular entry, demonstrating the usage of pAPN as a cross-
54 genus CoV functional receptor. The identification of PDCoV receptor provides another
55 example of the expanded host range of CoV, and paves the way for further investigation of
56 PDCoV-host interaction and pathogenesis.
57

58 **INTRODUCTION**

59 Coronaviruses (CoVs) are single-stranded, positive-sense RNA viruses with the largest
60 genome that cause mild or lethal respiratory and gastrointestinal diseases in humans and
61 animals (1). Currently, the subfamily *Coronavirinae* of the family *Coronaviridae* is classified
62 into four genera, *Alphacoronavirus*, *Betacoronavirus*, *Gammacoronavirus*, and
63 *Deltacoronavirus* (1). The fourth genus *Deltacoronavirus* has just been defined recently (2).
64 Since most of the GammaCoVs and DeltaCoVs are identified in avian species, birds are the
65 proposed original host for these two genera, whereas bats are considered as the original host
66 for the genera *Alphacoronavirus* and *Betacoronavirus* (2).

67 Porcine deltacoronavirus (PDCoV), in particular, was isolated from pigs in the United
68 States and many Asian countries including China, causing severe diarrhea, vomiting, and
69 dehydration in nursing piglets recently (3, 4). PDCoV and the other three emerging and re-
70 emerging swine enteric CoVs (SECoVs), including porcine epidemic diarrhea virus (PEDV),
71 transmissible gastroenteritis virus (TGEV), and a newly discovered swine enteric
72 alphacoronavirus (SeACoV) derived from the bat CoV HKU2 (5), have been causing a high
73 number of pig deaths and significant economic impacts, which are considered a serious threat
74 to the pork industry (3-7). PDCoV genomic RNA is approximately 25.4 kb in size. The
75 genome organization of PDCoV is similar to those of the other reported coronaviruses, with
76 the typical gene order 5'-ORF1a/1b-Spike (S)-Envelope (E)-Membrane (M)-NS6-
77 Nucleocapsid (N)/NS7-3' (2, 8). PDCoV is closely related to the sparrow CoV HKU17 (more
78 than 90% amino acid identities in all seven domains in ORF1a/1b) and they are believed to
79 be subspecies of the same species. Molecular clock analysis showed that the PDCoV jumped
80 from birds to mammals approximately 523 years ago (2).

81 Identification of cellular receptors used by CoV for binding and entry into host cells is
82 critical to understand pathogenesis and to develop intervention strategies. As of date, four
83 types of CoV functional protein receptors have been identified: (i) aminopeptidase N (APN)

for several AlphaCoVs including TGEV (9), (ii) carcinoembryonic antigen-related cell adhesion molecule 1 (CEACAM1), (iii) angiotensin converting enzyme 2 (ACE2), and (iv) dipeptidyl peptidase 4 (DPP4) for three distinct BetaCoVs, mouse hepatitis virus (MHV) (10), severe acute respiratory syndrome coronavirus (SARS-CoV) (11) and Middle East respiratory syndrome coronavirus (MERS-CoV) (12), respectively. Interestingly, the human ACE2 can also serve as the entry receptor for AlphaCoV human coronavirus (HCoV) NL63 in addition to SARS-CoV (13). These receptors interact with the amino-terminal receptor-binding domain S1 of specific CoV S glycoproteins, which determined the cross-species transmission and infection of CoVs (9-15).

While functional receptors for the representative members in *Alphacoronavirus* and *Betacoronavirus* have been continuously discovered, receptors for *Gammacoronavirus* and *Deltacoronavirus* are still unknown. In the current study, we demonstrate that, similar to ACE2, porcine APN (pAPN) acts as a cross-genus CoV functional receptor for both porcine DeltaCoV (PDCoV) and AlphaCoV (TGEV) based upon three lines of evidences. First, the soluble Fc-fusion S1 protein of PDCoV efficiently bound to the surface of target porcine cell lines known to express pAPN as TGEV-S1-Fc did, which could be blocked by soluble pAPN pre-treatment. Second, either PDCoV-S1 or TGEV-S1 physically recognized and interacted with pAPN by co-immunoprecipitation (IP) in pAPN-cDNA-transfected cells and by dot blot hybridization assay. Finally, exogenous expression of pAPN in refractory cells conferred susceptibility to PDCoV-S1 binding, and most importantly, for PDCoV entry and productive infection.

RESULTS

Soluble TGEV-S1 or PDCoV-S1 binding to porcine permissive cells endogenously expressing pAPN. It has been well known that swine testicular (ST) cells and porcine kidney epithelial LLC-PK1 cells are permissive for TGEV infection (9, 16). We noticed that PDCoV

was initially isolated and propagated in these two cell lines (3, 4), suggesting a common cell tropism of TGEV and PDCoV. In addition, neither African green monkey Vero cells (ATCC CCL-81) nor hamster BHK-21 cells are permissive for TGEV or PDCoV infection *in vitro* in our lab. To investigate whether PDCoV-S1 determines the cell tropism as that documented for TGEV-S1 (14), we generated the S1-human Fc (hFc) chimeric proteins from PDCoV (Chinese/Hunan strain; GenBank accession no. KY513724) and TGEV (prototype Purdue strain) (5), respectively. As expected, soluble TGEV-S1-hFc bound to target LLC-PK1 or ST cells, but not to non-susceptible Vero or BHK-21 cells by using flow cytometry analysis (Fig. 1A). Next we tested the binding of soluble PDCoV-S1 under the same conditions. Comparison of cellular surface binding of PDCoV-S1-hFc to LLC-PK1 or ST cells indicated significant similarities with TGEV-S1 binding, whereas S1-hFc binding was not detected in Vero or BHK-21 cells (Fig. 1B), which is correlated with infection of PDCoV.

We further confirmed that both LLC-PK1 and ST cells had endogenous expression of pAPN whereas Vero or BHK-21 cells lacked APN counterpart expression by western blotting (WB) analysis using a broadly reactive anti-APN antibody (Ab) (Fig. 1C). As controls, two stable cell lines Vero-pAPN and BHK-pAPN, both expressing pAPN, were established, by transfection with a recombinant construct, pAPN-Myc, expressing full-length pAPN cDNA fused with a Myc tag at the C-terminus, followed by selection with puromycin. Expression of pAPN was detected in Vero-pAPN cells (Fig. 1C). Comparison of APN expression between BHK-21 cells and BHK-pAPN had the similar result, showing pAPN expression only in BHK-pAPN cells (Fig. 1C). Thus, LLC-PK1 and ST cells are susceptible to both TGEV-S1 and PDCoV-S1 binding, permissive to both TGEV and PDCoV infection and express the TGEV receptor pAPN, whereas Vero and BHK-21 cells are not susceptible to binding, not permissive to infection and do not express APN.

Interaction between PDCoV-S1/TGEV-S1 and pAPN associated with cell tropism. The interaction between PDCoV-S1 and pAPN was analyzed by co-IP. BHK-21 cells were

136 transfected with PDCoV-S1-hFc or TGEV-S1-hFc expression construct alone, or an empty
137 vector expressing hFc alone, or co-transfected of each hFc construct with pAPN-Myc
138 plasmid. Expression of transfected Fc-tagged proteins and pAPN were confirmed in whole
139 cell lysates by WB with anti-Fc Ab and anti-Myc Ab, respectively (Fig. 2A, bottom). The
140 transfected BHK21 cells were then immunoprecipitated with Fc tag preadsorbed onto protein
141 A conjugated agarose beads. The bound protein complexes were subjected to WB analysis
142 with anti-Myc Ab or anti-Fc Ab. As shown in Fig. 2A (top), pAPN-Myc bound specifically
143 to either PDCoV-S1-hFc or TGEV-S1-hFc. In contrast, pAPN-Myc did not bind to the
144 control hFc protein (lanes 3 and 5). Notably, the amount of pAPN-Myc brought down by
145 PDCoV-S1-hFc (lane 4, top) was significantly less than that was brought down by TGEV-S1-
146 hFc (lane 6, top), whereas the expression level of pAPN-Myc is more abundant in lane 4 than
147 in lane 6. Since equal amounts of plasmid DNA of PDCoV-S1-hFc and TGEV-S1-hFc were
148 input for the IP experiment, as shown by no significant difference in the detection level
149 between S1-Fc proteins either in IP or in whole cell lysates (WCL) (Fig. 2A), the IP result
150 suggests that PDCoV-S1 may have a lower pAPN-binding affinity than TGEV-S1.

151 To further validate the specific interaction between PDCoV-S1 and pAPN, a dot blot
152 hybridization assay was conducted. It was shown that both TGEV-S1-hFc and PDCoV-S1-
153 hFc efficiently bound to the soluble pAPN ectodomain tagged with a mouse Fc (pAPN-mFc)
154 but not to the mFc control. On the other hand, the hFc bound to neither pAPN-mFc nor mFc
155 (Fig. 2B). These results demonstrated that either PDCoV-S1 or TGEV-S1 physically
156 recognized and interacted with pAPN.,

157 Next, the soluble pAPN-mFc or mFc was preincubated with TGEV-S1-hFc, PDCoV-S1-
158 hFc or hFc; the LLC-PK1 or ST cells were then subjected to flow cytometry analysis with the
159 mixtures as described in Fig. 1A and 1B. Treatment of S1-hFc with pAPN-mFc but not mFc
160 blocked surface binding (Fig. 3A), indicating that PDCoV-S1 or TGEV-S1 does employ
161 pAPN for cellular binding on host (swine) cells. These data collectively demonstrate a direct

and specific interaction between PDCoV-S1/TGEV-S1 and pAPN associated with cell tropism.

Exogenous pAPN expression in refractory Vero or BHK-21 cells confers susceptibility to PDCoV-S1 or TGEV-S1 binding. We next determined whether pAPN could indeed mediate PDCoV entry in refractory cells. The full-length cDNA encoding pAPN fused with a Myc tag (pAPN-Myc) was stably expressed by puromycin selection in Vero or BHK-21 cell lines (Vero-pAPN or BHK-pAPN), as shown by WB analysis (Fig. 1C). Furthermore, surface expression of pAPN on Vero-pAPN or BHK-pAPN was validated by detection of efficient binding of TGEV-S1-hFc or PDCoV-S1-hFc by flow cytometry analysis, which could be blocked by soluble pAPN-mFc pre-treatment (Fig. 3B), similar to what was observed in LLC-PK1 or ST cells (Fig. 3A). In contrast, the two S1-hFc did not bind to the parental cell lines (Fig. 3B), which was in line with the result in Fig. 1A and 1B. As controls, the two S1-hFc soluble proteins did not bind to Vero cells overexpressing the SARS-CoV and HCoV-NL63 receptor ACE2 (11, 13) or BHK-21 cells exogenously expressing ACE2 (Fig. 3B). Therefore, exogenous expression of pAPN in refractory Vero or BHK-21 cells conferred specific susceptibility to PDCoV-S1 or TGEV-S1 binding. In addition, cytoplasmic expression of pAPN in Vero-pAPN or BHK-pAPN was also validated by immunofluorescence assay (IFA) using anti-Myc Ab or anti-pAPN Ab (Fig. 4A).

Exogenous pAPN expression allows refractory cell lines to support PDCoV efficient replication and productive infection. The Vero, Vero-pAPN, BHK-21 and BHK-pAPN cell lines were inoculated with either TGEV or PDCoV at a multiplicity of infection (MOI) of 0.1, respectively. As expected, TGEV N protein antigens were detected and spread in the cytoplasm of 35-40% of either Vero-pAPN or BHK-pAPN cells by 36 h post-inoculation (hpi), but no viral antigens were found in challenged Vero or BHK-21 cells (Fig. 4A, top). PDCoV also infected Vero-pAPN cells with an efficiency of 25-30% or BHK-pAPN cells with an efficiency of 30-35%, but did not infect Vero or BHK-21 cells by 36 hpi, when

188 assessed by detection of specific PDCoV N protein expression (Fig. 4A, bottom). A slightly
189 lower infection efficiency of PDCoV than that of TGEV could likely be accounted for by the
190 possibly lower pAPN-binding affinity of PDCoV-S1 (Fig. 2A). Development of cytopathic
191 effects characterized by cell rounding, aggregation and subsequent detachment in PDCoV-
192 infected Vero-pAPN cells was observed (Fig. 4B).

193 To determine whether pAPN-expressing cells could confer PDCoV replication
194 competency, Vero-pAPN or PDCoV-target LLC-PK1 cells were inoculated with PDCoV
195 (MOI=0.1) with or without soluble pAPN pre-incubation, and the viral RNA in the
196 supernatant of cell lysates at 2, 8 and 24 hpi were assessed by quantitative RT-PCR,
197 respectively. Fig. 5 showed that PDCoV RNA was synthesized gradually from two types of
198 cells. Moreover, soluble pAPN pre-incubation with PDCoV blocked viral replication at the
199 early stage (2 and 8 hpi), indicating that replication-competent PDCoV utilizes pAPN as an
200 entry receptor (Fig. 5). At 24 hpi, inhibition of PDCoV replication by soluble pAPN was not
201 significant in both cell lines, suggesting that PDCoV is probably propagated and spread from
202 cell-to-cell by this time point (Fig. 5).

203 The progressive PDCoV release into the cultured medium ("extracellular") was
204 determined by dynamic viral RNA synthesis and virus titers. Both extracellular and
205 intracellular PDCoV RNA and extracellular virus titers could be detected in the supernatants
206 of Vero-pAPN and the control LLC-PK1 cells but not in the supernatants of Vero cells during
207 a period of 72 hpi (Fig. 6A and 6B), indicating RNA replication and a productive PDCoV
208 infection of Vero-pAPN cells. Since the extracellular PDCoV infectious titers were assessed
209 on fresh LLC-PK1 cells by endpoint dilutions (titration), the result also demonstrated that
210 PDCoV secreted from Vero-pAPN cells could be passaged (Fig. 6B). Progeny PDCoV
211 infection of fresh LLC-PK1 cells was also validated by IFA using an anti-PDCoV-N Ab (Fig.
212 6C). The PDCoV growth curve in Vero-pAPN cells was lower than that in control LLC-PK1

cells; but reached the peak titers in the period of 48-72 hpi (5.12 $\log_{10}$TCID$_{50}$/ml and 6.27 $\log_{10}$TCID$_{50}$/ml, respectively)

For comparison of infection efficiency, we also determined the growth kinetics of TGEV secreted from Vero-pAPN, Vero or from control LLC-PK1 cells on fresh LLC-PK1 cells (Fig. 6B). No TGEV was produced in Vero cells. In control LLC-PK1 cells, extracelluar TGEV had a growth curve with virus titers analogous to extracelluar PDCoV, while for Vero-pAPN cells inoculated with either TGEV or PDCoV, extracelluar TGEV propagated more efficiently than extracelluar PDCoV, reaching a peak titer at 48 hpi (5.67 $\log_{10}$TCID$_{50}$/ml), and with approximately 3- to 10-fold higher titers during 6-48 hpi (Fig. 6B). The kinetics data was consistent with the distinct expression level of N proteins between TGEV and PDCoV (Fig. 4A).

Theses results collectively demonstrated that exogenous expression of recombinant pAPN in refractory cell lines is sufficient to allow binding, entry, synthesis of viral RNA and protein and release of infectious PDCoV. Therefore, pAPN serves as a functional receptor for both PDCoV and TGEV.

DISCUSSION

Identification of the host functional receptor for a pathogenic virus is very important for understanding the mechanisms of virus-host interplay. APN, also known as a type II zinc metalloprotease, mediates the entry of most of AlphaCoVs (9, 17, 18). Our study indicated that PDCoV in the newly defined *Deltacoronavirus* genus engages the same pAPN receptor, which is expressed in abundance in the porcine small intestinal mucosa, to infect the same target cells as TGEV (9), likely leading to induction of clinical signs of diarrhea in piglets. The highly conserved feature of receptor engagement between PDCoV and TGEV is consistent with a closely molecular architecture of the S glycoproteins (19), common cell

238 tropism (4, 9, 16) and consequent pathogenesis exhibited by these two SECoVs in distinct
239 CoV genus (3).

240 Intriguingly, among four pathogenic SECoVs, the AlphaCoV PEDV was previously
241 reported to utilize pAPN as an entry receptor by using a pseudotype assay with PEDV S
242 protein (20). However, recent studies have demonstrated that, none of the pAPN, human
243 APN (hAPN), or green monkey APN is a functional receptor for PEDV in cultured porcine,
244 human or Vero cells (21-23). Moreover, we found that a recombinant PEDV expressing GFP,
245 PEDV-GFP (23), and other Chinese and U.S. genogroup-1 and genogroup-2 PEDV strains
246 (6, 24, 25) did not infect BHK-21 or BHK-pAPN cells (data not shown). Since BHK-21 is the
247 refractory cell line to infection of PEDV, TGEV and PDCoV; but it can support PEDV
248 replication and production by transfection of PEDV infectious cDNA clones (unpublished
249 data), the comparative results reveal that BHK-pAPN cells conferred TGEV and PDCoV but
250 not PEDV infection. This provides an additional evidence of exclusive engagement of pAPN
251 for PDCoV and TGEV.

252 Most recently, our lab discovered a novel bat-CoV-HKU2-related swine enteric virus,
253 SeACoV, in southern China (5). The SeACoV is unique since it has an AlphaCoV genomic
254 backbone with an S gene phylogenetically related to that from BetaCoV (5). Members of
255 BetaCoV have not been found to use APN as receptor, and SeACoV infects monkey-APN-
256 deficient Vero cells as PEDV does (5), suggesting that APN is likely not the entry receptor
257 for SeACoV.

258 TGEV infection is highly natural host specific *in vitro* and *in vivo*, in that TGEV uses
259 pAPN but not hAPN as its cellular receptor. A related human AlphaCoV, HCoV-229E,
260 utilizes hAPN but not pAPN to enter host cells (17, 26). Mutagenesis study and subsequent
261 determination of the crystal structure of pAPN revealed that different virus-binding motifs
262 (VBMs) in pAPN/hAPN containing species-specific *N*-linked glycan are required to mediate
263 susceptibility to infection with TGEV and HCoV-229E (27, 28). TGEV recognizes APN

residues 728–744 (VBM2) whereas HCoV-229E recognizes residues 283–292 (VBM1); both regions are located on the outer surface of APN and can be approached easily by viruses (27). Furthermore, the crystal structure of porcine respiratory CoV (PRCV; a TGEV variant) receptor-binding domain (RBD) on S1 in complex with pAPN revealed that Tyr-304 and Trp-347 residues at the two RBD protruding tips penetrate small cavities of the APN domain DIV (containing VBM2), and the other RBD residues contact an N-acetyl glucosamine linked to Asn-736 of pAPN, which are critical for PRCV/TGEV binding to APN (29). The absence of an APN-binding Tyr and a different conformation of the receptor-binding loop at the tip in HCoV-229E RBD are in line with a distinct VBM (e.g. VBM1) recognized by HCoV-229E, although the structure of complex of HCoV-229E RBD and hAPN has not yet been resolved. More recently, a near atomic-resolution cryo-electron microscopy structure of PDCoV S glycoprotein trimer has revealed that the PDCoV RBD displays a β–sandwich fold reminiscent of that of AlphaCoVs, harboring topologically similar glycosylation sites on the β-sandwich surface (19). Several aromatic residues (Phe-318, Tyr-394, Trp-396 and Tyr-398) at the protruding tips have also been speculated to mediate receptor-RBD interaction (19).

However, since PDCoV can also infect some human cell lines such as Huh-7 expressing hAPN *in vitro* (preliminary data not shown), and calves *in vivo* (30), and could be detected in Asian leopard cats and Chinese ferret badgers (31), we hypothesize that PDCoV can utilize APNs from the other mammalian species as the receptor, which distinguishes TGEV and HCoV-229E in usage of host-specific APN. If so, the VBM in APN recognized by PDCoV-S1 may be different from VBM1 by HCoV-229E or VBM2 recognized by TGEV. This hypothesis is also supported by the experimental data from this study, where we found that the results of co-IP, IFA and comparative growth kinetics (Fig. 2A, Fig. 4A and Fig. 6B) indicated the likely differences in receptor-binding affinity and in consequent infection efficiency in Vero-pAPN cells between PDCoV and TGEV. If so, the structural basis for this APN-binding by cross-genus CoVs is totally distinct from what have been known for ACE2-

290 binding by SARS-CoV and HCoV-NL63 (32, 33). In the latter case, SARS-CoV does not
291 have homologous structure in the RBD core with HCoV-NL63; but both viruses recognize a
292 "virus-binding hotspot" in the common ACE2 region (32). Future studies on mapping of the
293 PDCoV-binding VBM in pAPN and resolving the structure of PDCoV-RBD in complex with
294 pAPN, are warranted to confirm our hypothesis.

295 Since *Deltacoronavirus* is believed to originate from avian CoVs (2), our result also
296 raises a question whether the APN counterparts in avian species play a role in PDCoV cross-
297 species transmission. Nevertheless, the present study suggests that PDCoV has evolved a
298 mechanism that utilizes pAPN as its entry receptor to expand host range. The identification of
299 pAPN as a functional receptor used by PDCoV paves the way for dissecting the molecular
300 mechanisms of PDCoV-host interactions and pathogenesis as well as facilitates future
301 vaccine development and intervention strategies against PDCoV infection.

302

303 **MATERIALS AND METHODS**

304 **Cell lines, virus stocks and viral antibodies.** A porcine kidney epithelial cell line LLC-
305 PK1 (ATCC CL-101), a swine testis cell line ST (ATCC CRL-1746), a baby hamster kidney
306 fibroblast cell line BHK-21 (ATCC CCL-10), and an African green monkey kidney epithelial
307 Vero cell (ATCC CCL-81) were individually grown in Dulbecco's modified Eagle's medium
308 (DMEM) supplemented with 10% fetal bovine serum (FBS) and 1% antibiotics (penicillin,
309 streptomycin, w/v). All cells were grown at 37°C with 5% CO_2.

310 The TGEV Purdue strain (a gift from Dr. Rong Ye at Shanghai Medical College of
311 Fudan University, China) was produced in ST cells, whereas the PDCoV CH/Hunan/2014
312 strain (GenBank accession no. KY513724) was propagated in LLC-PK1 cells (5). ST or
313 LLC-PK1 cells were seeded at 70% confluency in T-25 flasks and incubated overnight. After
314 washing the cells with PBS, viruses at MOI = 0.1 were added to each flask. After 2 h
315 incubation at 37 °C, the cells were washed with PBS and then cultured in DMEM without

316 FBS. Cells were observed daily to check for any cytopathic effect (CPE). When CPE was
317 obvious, whole cell cultures (supernatant and cells) were harvested and subjected to three
318 freeze-thaw cycles prior to removal of cell debris by centrifugation. The virus titers of TGEV
319 or PDCoV were determined by endpoint dilutions as 50% tissue culture infective dose
320 ($TCID_{50}$) on fresh cells as described previously (24). Virus stocks were stored at -80°C until
321 use.

322 Anti-PDCoV-nucleocapsid (N) monoclonal antibody (mAb) was purchased from
323 Medgene Labs (Brookings, SD, USA), whereas anti-TGEV-N polyclonal antibody (pAb) was
324 generated in-house. Briefly, the full-length N protein of TGEV with a 6 × histidine tag
325 expressed in *E. coli* was purified and used to immunize two New Zealand White rabbits.
326 Antisera were harvested and affinity purified at 55 days postimmunization.

327 **Construction of the recombinant plasmids.** The complete coding region of porcine
328 APN (pAPN; GenBank accession no. KX342854) was amplified by one-step RT-PCR using
329 total RNAs extracted from porcine small intestine, and subsequently cloned into a pCI-neo
330 vector (Promega, USA) using NheI and SalI restriction sites. The recombinant plasmid was
331 designated as pCI-pAPN (23). Expression of pAPN protein *in vitro* was confirmed by
332 transiently transfection of pCI-pAPN in BHK-21 or Vero cells by immunofluorescence assay
333 (IFA) with an anti-APN pAb (Abcam #93897) (23). Next, the pAPN ectodomain encoding
334 amino acid (aa) 62-963 (27) was amplified from pCI-pAPN and inserted into a pFUSE-
335 mIgG1-Fc2 vector (Invivogen, USA) containing an in-frame C-terminal murine IgG1 Fc
336 (mFc) fragment, to construct an expression construct named pAPN-mFc. The third pAPN-
337 expressing construct, pAPN-Myc, harboring the full-length pAPN cDNA fused with a Myc
338 tag at the C-terminus, was engineered between XhoI and HpaI restriction sites in a lentiviral
339 vector pLV-CMV-PURO (kindly provided by Prof. Pinglong Xu at Life Sciences Institute of
340 Zhejiang University). For construction of soluble human IgG1 Fc (hFc) fusion proteins,
341 TGEV-S1 (aa 1-832) and PDCoV-S1 (aa 1-574) subunits were amplified by PCR from the

342 respective full-length cDNA of the viral genome and inserted into a pFUSE-hIgG1-Fc1
343 vector (Invivogen, USA). The recombinant plasmids were designated as pFUSE-TGEV-S1-
344 hFc and pFUSE-PDCoV-S1-hFc. The expression plasmid harboring the full-length cDNA of
345 the SARS-CoV cellular receptor ACE2, pCMV3-Flag-ACE2 (#HG10108-NF), was
346 purchased from Sino Biological Inc. (Beijing, China).

347 **Generation of two stable cell lines expressing pAPN.** Two stable cell lines, Vero-
348 pAPN and BHK-pAPN, were established in Vero and BHK-21 cells by transfection with the
349 construct pAPN-Myc followed by selection with 10 μg/ml of puromycin, respectively,
350 according to described previously (34). Expression of pAPN-Myc fusion protein was
351 confirmed by IFA with an anti-Myc mAb (Cell Signaling Technology, #2276) and an anti-
352 APN pAb. PDCoV or TGEV was inoculated and cultured in Vero-pAPN, Vero, BHK-pAPN
353 or BHK-21 cells in the presence of trypsin (3 μg/ml; Sigma).

354 **Flow cytometry analysis.** We followed the protocol as described previously in ref. (21).
355 Briefly, soluble hFc and mFc fusion proteins (TGEV-S1-hFc, PDCoV-S1-hFc, hFc, mFc and
356 pAPN-mFc) were transiently expressed in 293T cells and affinity purified from the
357 supernatant medium using protein A sepharose beads (Transbionovo, Beijing, China),
358 respectively. Analysis of purified proteins was performed by sodium dodecyl sulfate
359 polyacrylamide gel electrophoresis (SDS-PAGE) to ensure the purity and quality (data not
360 shown). Binding of soluble Fc proteins to surface of given cells was performed by incubation
361 with 10 μg/ml of purified S1-hFc proteins followed by detection with a FITC-conjugated
362 anti-human IgG Fc Ab (Thermo Fisher Scientific) by flow cytometer. Blocking of S1-hFc
363 was performed by preincubation with soluble pAPN-mFc or mFc for 2 h prior to conducting
364 surface binding assay.

365 **Immunofluorescence assay, western blot and dot blot hybridization assay.** Plasmids
366 were transiently transfected into Vero or BHK-21 cells using Lipofectamine 3000 (Thermo
367 Fisher Scientific) according to the manufacturer's protocol. Transfected cells or virus-

368 infected cells were cultured for 36 to 72 hours, and then applied to immunofluorescence
369 assay, co-IP or western blot to detect protein expression or interaction. For IFA, cells were
370 washed twice with phosphate-buffered saline (PBS) and fixed with acetone. Cells were then
371 incubated with the primary Ab. After incubation for 1 hour at room temperature, the cells
372 were washed with PBS and stained with the secondary Ab followed by 4', 6-diamidino-2-
373 phenylindole (DAPI) staining. For western blot analysis, cells were lysed in 125 μl CelLytic
374 M lysis buffer (Sigma) per 10^6 cells. The whole cell lysates (WCL) was preadsorbed onto
375 protein A conjugated agarose beads prior to SDS-PAGE for co-IP analysis, or was used for
376 SDS-PAGE directly. Samples were resolved on SDS-PAGE and transferred onto
377 polyvinylidene difluoride (PVDF) membrane that was subsequently blocked with Tris-
378 buffered saline (TBS) containing 3% bovine serum albumin (BSA) overnight at 4°C. Proteins
379 were detected using the primary Ab followed by incubation with horseradish peroxidase
380 (HRP)-conjugated secondary Ab (Thermo Fisher Scientific). Binding of Fc-tagged proteins
381 (TGEV-S1-hFc, PDCoV-S1-hFc or hFc) to soluble pAPN-mFc or mFc was detected by dot
382 blot hybridization assay as described by Li *et al* (21).

383 **Quantitative RT-PCR.** Total RNA was extracted from supernatant medium and cell
384 lysates of PDCoV-inoculated cells at different time points using an AxyPrep Multisource
385 Total RNA Miniprep Kit (Axygen). PDCoV RNA titer was monitored by one-step qRT-PCR
386 targeting the membrane (M) gene with the primers (5'-ATCGACCACATGGCTCCAA-3'
387 and 5'-CAGCTCTTGCCCATGTAGCTT-3') and the probe, FAM-
388 CACACCAGTCGTTAAGCATGGCAAGCT-BHQ) as described previously (35, 36).
389 Standard curves were performed to allow absolute quantitation of PDCoV RNA copy
390 numbers based upon the levels of *in-vitro*-transcribed RNA containing the targeting
391 sequences. Samples with a cycle threshold value of <35 were considered positive based upon
392 validation data using the standard RNA.

ACKNOWLEDGMENTS

This work was supported by the National Key Research and Development Program of China (2016YFD0500102), the National Natural Science Foundation of China (31572518), the Key Research and Development Program of Zhejiang province (2015C02021), the Thousand Young Talent Program of China, and the Zhejiang Provincial Science Foundation for Distinguished Young Scholars (LR14C180001). We thank Novoprotein Inc. (Shanghai, China) for assistance in protein purification.

References

1. **de Groot RJ, Baker SC, Baric R, Enjuanes L, Gorbalenya AE, Holmes KV, Perlman S, Poon L, Rottier PJM, Talbot PJ, Woo PCY, Ziebuhr J.** 2011. Coronaviridae, p 806-828. *In* King AMQ, Adams MJ, Carstens EB, Lefkowitz EJ (ed), Virus taxonomy : ninth report of the International Committee on Taxonomy of Viruses. Elsevier Academic Press, London.
2. **Woo PC, Lau SK, Lam CS, Lau CC, Tsang AK, Lau JH, Bai R, Teng JL, Tsang CC, Wang M, Zheng BJ, Chan KH, Yuen KY.** 2012. Discovery of seven novel Mammalian and avian coronaviruses in the genus deltacoronavirus supports bat coronaviruses as the gene source of alphacoronavirus and betacoronavirus and avian coronaviruses as the gene source of gammacoronavirus and deltacoronavirus. J Virol **86:**3995-4008.
3. **Jung K, Hu H, Saif LJ.** 2016. Porcine deltacoronavirus infection: Etiology, cell culture for virus isolation and propagation, molecular epidemiology and pathogenesis. Virus Res **226:**50-59.

4. **Ma Y, Zhang Y, Liang X, Lou F, Oglesbee M, Krakowka S, Li J.** 2015. Origin, evolution, and virulence of porcine deltacoronaviruses in the United States. MBio **6:**e00064.

5. **Pan Y, Tian X, Qin P, Wang B, Zhao P, Yang YL, Wang L, Wang D, Song Y, Zhang X, Huang YW.** 2017. Discovery of a novel swine enteric alphacoronavirus (SeACoV) in southern China. Veterinary Microbiology **211:**15-21.

6. **Huang YW, Dickerman AW, Pineyro P, Li L, Fang L, Kiehne R, Opriessnig T, Meng XJ.** 2013. Origin, evolution, and genotyping of emergent porcine epidemic diarrhea virus strains in the United States. MBio **4:**e00737-00713.

7. **Tian PF, Jin YL, Xing G, Qv LL, Huang YW, Zhou JY.** 2014. Evidence of recombinant strains of porcine epidemic diarrhea virus, United States, 2013. Emerg Infect Dis **20:**1735-1738.

8. **Wang YW, Yue H, Fang W, Huang YW.** 2015. Complete Genome Sequence of Porcine Deltacoronavirus Strain CH/Sichuan/S27/2012 from Mainland China. Genome Announc **3:**e00945-00915.

9. **Delmas B, Gelfi J, L'Haridon R, Vogel LK, Sjostrom H, Noren O, Laude H.** 1992. Aminopeptidase N is a major receptor for the entero-pathogenic coronavirus TGEV. Nature **357:**417-420.

10. **Williams RK, Jiang GS, Holmes KV.** 1991. Receptor for mouse hepatitis virus is a member of the carcinoembryonic antigen family of glycoproteins. Proc Natl Acad Sci U S A **88:**5533-5536.

11. **Li W, Moore MJ, Vasilieva N, Sui J, Wong SK, Berne MA, Somasundaran M, Sullivan JL, Luzuriaga K, Greenough TC, Choe H, Farzan M.** 2003. Angiotensin-converting enzyme 2 is a functional receptor for the SARS coronavirus. Nature **426:**450-454.

12. **Raj VS, Mou H, Smits SL, Dekkers DH, Muller MA, Dijkman R, Muth D, Demmers JA, Zaki A, Fouchier RA, Thiel V, Drosten C, Rottier PJ, Osterhaus AD, Bosch BJ, Haagmans BL.** 2013. Dipeptidyl peptidase 4 is a functional receptor for the emerging human coronavirus-EMC. Nature **495:**251-254.

13. **Hofmann H, Pyrc K, van der Hoek L, Geier M, Berkhout B, Pohlmann S.** 2005. Human coronavirus NL63 employs the severe acute respiratory syndrome coronavirus receptor for cellular entry. Proc Natl Acad Sci U S A **102:**7988-7993.

14. **Godet M, Grosclaude J, Delmas B, Laude H.** 1994. Major receptor-binding and neutralization determinants are located within the same domain of the transmissible gastroenteritis virus (coronavirus) spike protein. J Virol **68:**8008-8016.

15. **Delmas B, Gelfi J, Kut E, Sjostrom H, Noren O, Laude H.** 1994. Determinants essential for the transmissible gastroenteritis virus-receptor interaction reside within a domain of aminopeptidase-N that is distinct from the enzymatic site. J Virol **68:**5216-5224.

16. **Rossen JW, Bekker CP, Voorhout WF, Strous GJ, van der Ende A, Rottier PJ.** 1994. Entry and release of transmissible gastroenteritis coronavirus are restricted to apical surfaces of polarized epithelial cells. J Virol **68:**7966-7973.

17. **Yeager CL, Ashmun RA, Williams RK, Cardellichio CB, Shapiro LH, Look AT, Holmes KV.** 1992. Human aminopeptidase N is a receptor for human coronavirus 229E. Nature **357:**420-422.

18. **Tresnan DB, Levis R, Holmes KV.** 1996. Feline aminopeptidase N serves as a receptor for feline, canine, porcine, and human coronaviruses in serogroup I. J Virol **70:**8669-8674.

19. **Xiong X, Tortorici MA, Snijder J, Yoshioka C, Walls AC, Li W, McGuire AT, Rey FA, Bosch BJ, Veesler D.** 2017. Glycan shield and fusion activation of a

467 deltacoronavirus spike glycoprotein fine-tuned for enteric infections. J Virol
468 **92:**e01628-01617.

469 20. **Liu C, Tang J, Ma Y, Liang X, Yang Y, Peng G, Qi Q, Jiang S, Li J, Du L, Li F.**
470 2015. Receptor usage and cell entry of porcine epidemic diarrhea coronavirus. J Virol
471 **89:**6121-6125.

472 21. **Li W, Luo R, He Q, van Kuppeveld FJM, Rottier PJM, Bosch BJ.** 2017.
473 Aminopeptidase N is not required for porcine epidemic diarrhea virus cell entry.
474 Virus Res **235:**6-13.

475 22. **Shirato K, Maejima M, Islam MT, Miyazaki A, Kawase M, Matsuyama S,**
476 **Taguchi F.** 2016. Porcine aminopeptidase N is not a cellular receptor of porcine
477 epidemic diarrhea virus, but promotes its infectivity via aminopeptidase activity. J
478 Gen Virol **97:**2528-2539.

479 23. **Ji CM, Wang B, Zhou J, Huang YW.** 2018. Aminopeptidase-N-independent entry
480 of porcine epidemic diarrhea virus into Vero or porcine small intestine epithelial cells.
481 Virology **517:**16-23.

482 24. **Qin P, Li H, Wang JW, Wang B, Xie RH, Xu H, Zhao LY, Li L, Pan Y, Song Y,**
483 **Huang YW.** 2017. Genetic and pathogenic characterization of a novel reassortant
484 mammalian orthoreovirus 3 (MRV3) from a diarrheic piglet and seroepidemiological
485 survey of MRV3 in diarrheic pigs from east China. Veterinary Microbiology
486 **208:**126-136.

487 25. **Zhao P, Wang B, Ji CM, Cong X, Wang M, Huang YW.** 2018. Identification of a
488 peptide derived from the heptad repeat 2 region of the porcine epidemic diarrhea virus
489 (PEDV) spike glycoprotein that is capable of suppressing PEDV entry and inducing
490 neutralizing antibodies. Antiviral Res **150:**1-8.

26. **Kolb AF, Maile J, Heister A, Siddell SG.** 1996. Characterization of functional domains in the human coronavirus HCV 229E receptor. J Gen Virol **77 (Pt 10):**2515-2521.

27. **Chen L, Lin YL, Peng G, Li F.** 2012. Structural basis for multifunctional roles of mammalian aminopeptidase N. Proc Natl Acad Sci U S A **109:**17966-17971.

28. **Wentworth DE, Holmes KV.** 2001. Molecular determinants of species specificity in the coronavirus receptor aminopeptidase N (CD13): influence of N-linked glycosylation. J Virol **75:**9741-9752.

29. **Reguera J, Santiago C, Mudgal G, Ordono D, Enjuanes L, Casasnovas JM.** 2012. Structural bases of coronavirus attachment to host aminopeptidase N and its inhibition by neutralizing antibodies. PLoS Pathog **8:**e1002859.

30. **Jung K, Hu H, Saif LJ.** 2017. Calves are susceptible to infection with the newly emerged porcine deltacoronavirus, but not with the swine enteric alphacoronavirus, porcine epidemic diarrhea virus. Arch Virol **162:**2357-2362.

31. **Dong BQ, Liu W, Fan XH, Vijaykrishna D, Tang XC, Gao F, Li LF, Li GJ, Zhang JX, Yang LQ, Poon LL, Zhang SY, Peiris JS, Smith GJ, Chen H, Guan Y.** 2007. Detection of a novel and highly divergent coronavirus from asian leopard cats and Chinese ferret badgers in Southern China. J Virol **81:**6920-6926.

32. **Wu K, Li W, Peng G, Li F.** 2009. Crystal structure of NL63 respiratory coronavirus receptor-binding domain complexed with its human receptor. Proc Natl Acad Sci U S A **106:**19970-19974.

33. **Li F, Li W, Farzan M, Harrison SC.** 2005. Structure of SARS coronavirus spike receptor-binding domain complexed with receptor. Science **309:**1864-1868.

34. **Huang YW, Dryman BA, Li W, Meng XJ.** 2009. Porcine DC-SIGN: molecular cloning, gene structure, tissue distribution and binding characteristics. Dev Comp Immunol **33:**464-480.

35. **Marthaler D, Raymond L, Jiang Y, Collins J, Rossow K, Rovira A.** 2014. Rapid detection, complete genome sequencing, and phylogenetic analysis of porcine deltacoronavirus. Emerg Infect Dis **20:**1347-1350.

36. **Wang J, Lei X, Qin P, Zhao P, Wang B, Wang Y, Li Y, Jin H, Li L, Huang YW.** 2017. [Development and application of real-time RT-PCR and S1 protein-based indirect ELISA for porcine deltacoronavirus]. Sheng Wu Gong Cheng Xue Bao **33:**1265-1275.

526 # FIGURE LEGENDS

527

528 **Figure 1.** Soluble TGEV-S1 or PDCoV-S1 binds to porcine permissive cells endogenously
529 expressing pAPN. (A) Binding of soluble TGEV S1 protein to cellular surface by flow
530 cytometry analysis. Equal amounts (10 μg/ml) of TGEV-S1-hFc (filled histogram) or hFc
531 (dashed line) were incubated with susceptible LLC-PK1 or ST cells, or non-susceptible Vero
532 or BHK-21 cells. Cellular surface binding was detected by a FITC-conjugated anti-human
533 IgG Fc. (B) Binding of soluble PDCoV S1 to LLC-PK1, ST cells, Vero or BHK-21 cells.
534 Equal amounts (10 μg/ml) of PDCoV-S1-hFc (filled histogram) or Fc only (dashed line) were
535 incubated with four cell lines, followed by a FITC-conjugated anti-human IgG Fc detection.
536 (C) Detection of endogenous expression of pAPN on LLC-PK1 or ST cells, or pAPN
537 exogenous expression on Vero-pAPN or BHK-pAPN stable cells by immunobloting analysis
538 using an anti-APN Ab.

539

540 **Figure 2.** PDCoV-S1 or TGEV-S1 interacts with pAPN. (A) BHK-21 cells were transfected
541 with equal amounts (2 μg) of the empty vector pFUSE-Fc alone, pFUSE-Fc and pAPN-Myc
542 (with a C-terminal Myc-tag), PDCoV-S1-Fc alone, PDCoV-S1-Fc and pAPN-Myc, TGEV-
543 S1-Fc alone, and TGEV-S1-Fc and pAPN-Myc, respectively. The whole cell lysates (WCL)
544 was preadsorbed onto protein A conjugated agarose beads prior to SDS-PAGE for co-IP
545 analysis, or was used for SDS-PAGE directly. The protein complex was detected by using an
546 HRP-conjugated anti-Myc Ab and an HRP-conjugated anti-Fc Ab. (B) Detection of binding
547 of human Fc-tagged proteins (TGEV-S1-hFc, PDCoV-S1-hFc or hFc) to soluble pAPN by
548 dot blot hybridization assay. Porcine APN ectodomain tagged with a C-terminal murine IgG1
549 Fc (pAPN-mFc) or mFc was spotted on nitrocellulose membrane. Binding of S1-hFc proteins
550 to pAPN was detected by using an HRP-conjugated anti-human Fc Ab.

551

552 **Figure 3.** Flow cytometry analysis of cellular surface expression of pAPN. (A) Soluble
553 pAPN-mFc (10 μg/ml) pre-incubation was able to block TGEV-S1-hFc or PDCoV-S1-hFc
554 binding to permissive LLC-PK1 or ST cells (grey-filled histogram), whereas 10 μg/ml of
555 soluble mFc pre-incubation did not block TGEV-S1-hFc or PDCoV-S1-hFc binding (black-
556 filled histogram). Pre-incubation of pAPN-mFc followed by hFc binding was used as the
557 control (dashed line). Cellular surface binding was each detected by a FITC-conjugated anti-
558 human IgG Fc. (B) TGEV-S1-hFc or PDCoV-S1-hFc bound to BHK-21 or Vero cells stably
559 expressing pAPN (BHK-pAPN or Vero-pAPN; red histogram) but not to BHK-21, Vero
560 (green histogram), BHK-21 expressing ACE2, or Vero expressing ACE2 cells (blue
561 histogram). Soluble pAPN-mFc (10 μg/ml) pre-incubation was able to block TGEV-S1-hFc
562 or PDCoV-S1-hFc binding to BHK-pAPN or Vero-pAPN cells (yellow histogram). Cellular
563 surface binding was detected as described in Fig. 1A and 1B.

564

565 **Figure 4.** Vero or BHK-21 cells stably expressing pAPN confer susceptibility to PDCoV or
566 TGEV infection. (A) Vero, Vero-pAPN, BHK-21 and BHK-pAPN cells were challenged
567 with TGEV or PDCoV, respectively. At 36 hours post-challenge, TGEV-challenged cells
568 were co-stained with a rabbit anti-TGEV-N pAb and a mice anti-Myc mAb, whereas
569 PDCoV-challenged cells were co-stained with a mice anti-PDCoV-N mAb and a rabbit anti-
570 APN pAb. Alexa Fluor 488- or 594-conjugated anti-rabbit or anti-mice IgG were co-stained
571 for secondary antibody detection followed by DAPI incubation. Magnification = 200×. (B)
572 Evidence of PDCoV infection in Vero-pAPN cells showing cytopathic effects (CPE) with
573 cell rounding and aggregation (indicated by red arrows) at 36 h post-infection.

574

575 **Figure 5.** Infection of PDCoV in LLC-PK1 or Vero-pAPN cells was inhibited by soluble
576 pAPN (at a concentration of 39 or 78 μg/ml) within 24 hours. PDCoV RNA titers were
577 measured by one-step quantitative RT-PCR targeting the M gene. *$P < 0.05$, **$P < 0.01$.
578
579 **Figure 6.** Determination of the kinetics of PDCoV replication, propagation and release in
580 Vero-pAPN or control LLC-PK1 cells. (A) The amounts of extracellular and intracellular
581 viral RNA in Vero-pAPN, Vero and LLC-PK1 cells were assessed in triplicate by qRT-PCR,
582 respectively. (B) Virus titers ($TCID_{50}$/ml) of PDCoV or TGEV released into the supernatant
583 of inoculated Vero-pAPN, Vero or LLC-PK1 cells were determined in triplicate on fresh
584 LLC-PK1 cells. Samples of supernatants and cells were collected at intervals between 2 to 72
585 hours post-inoculation. Error bars indicate standard deviation. (C) Infection of fresh LLC-
586 PK1 cells with progeny PDCoV collected from Vero-pAPN cells inoculated with PDCoV.
587 IFA was performed at 36 hpi. The expression of PDCoV N protein was detected by staining
588 with anti-PDCoV-N mAb and Alexa Fluor 488-conjugated goat anti-mouse IgG Ab (the
589 middle panel).

Fig. 1

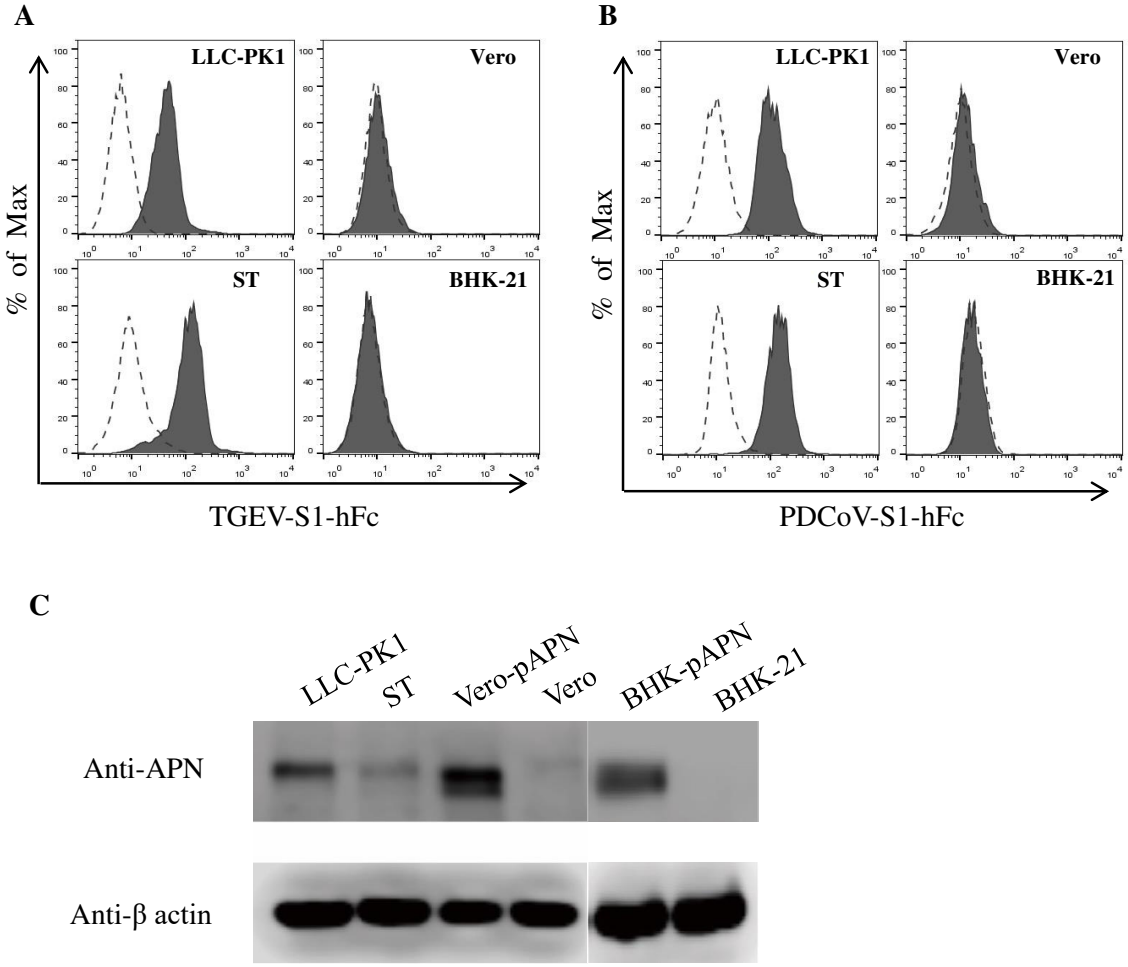

Fig. 2

A

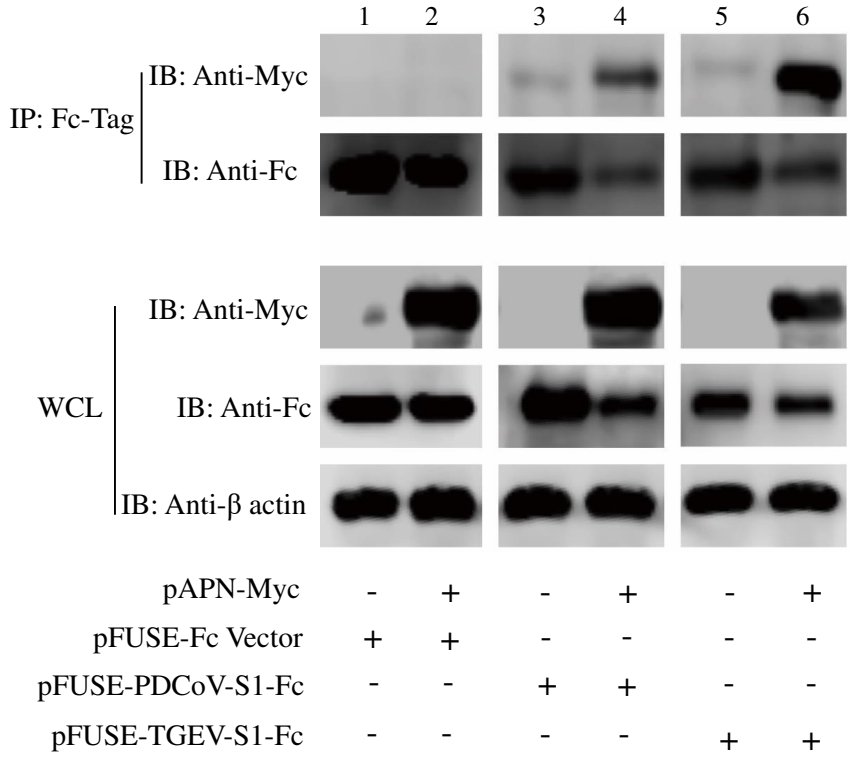

B

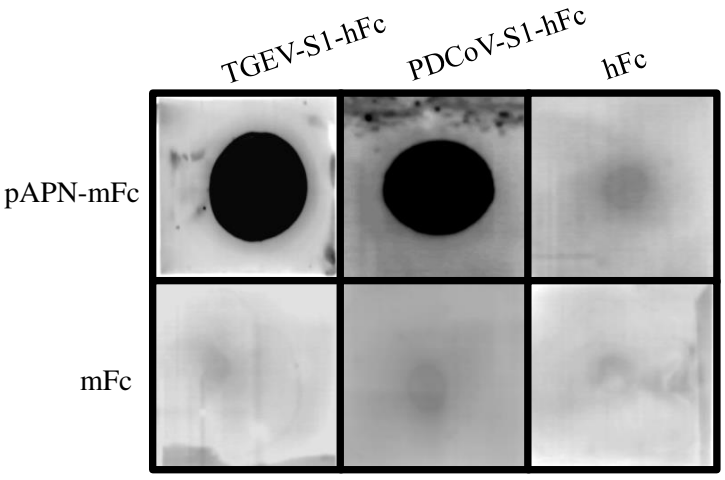

Fig. 3

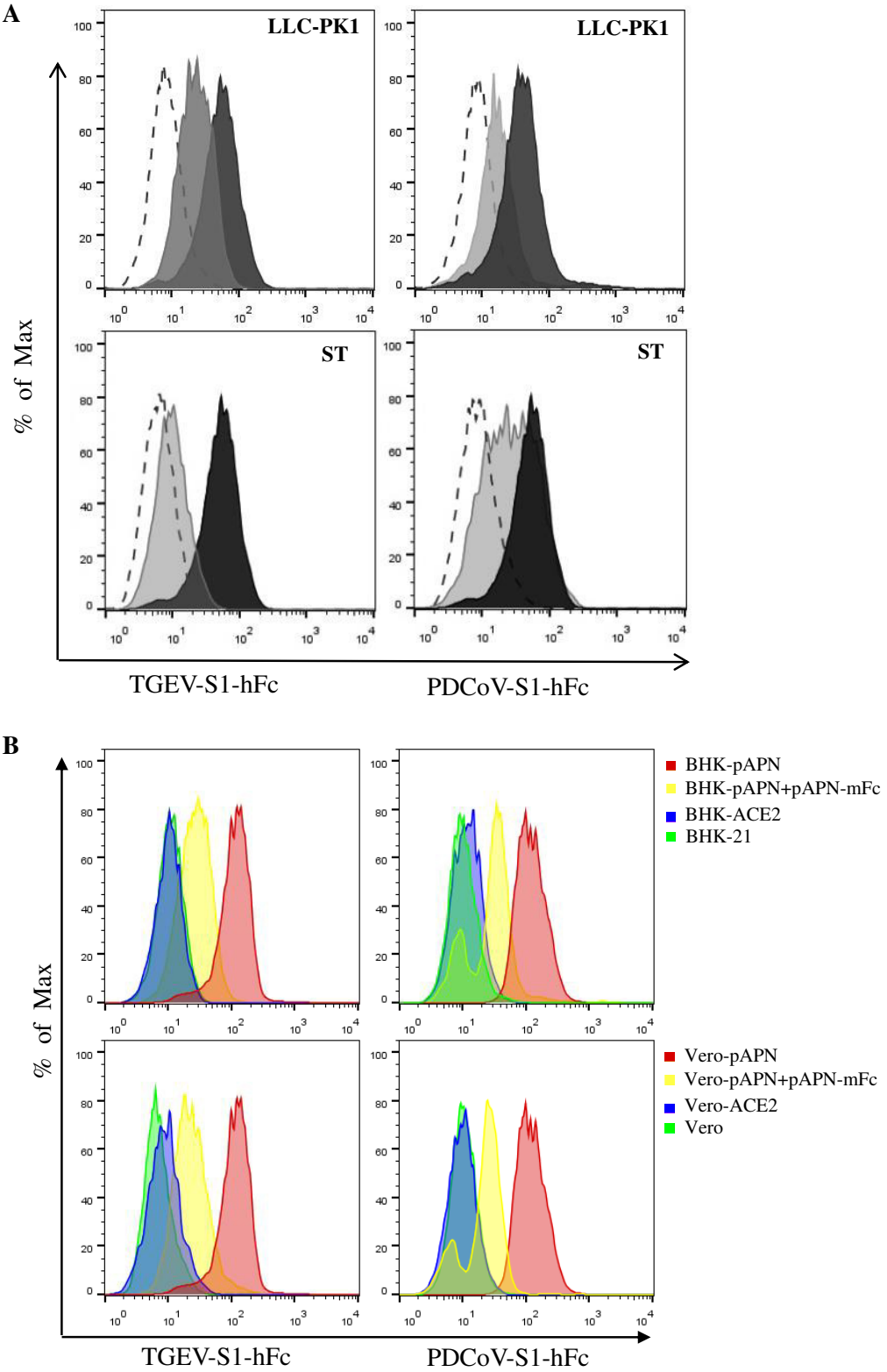

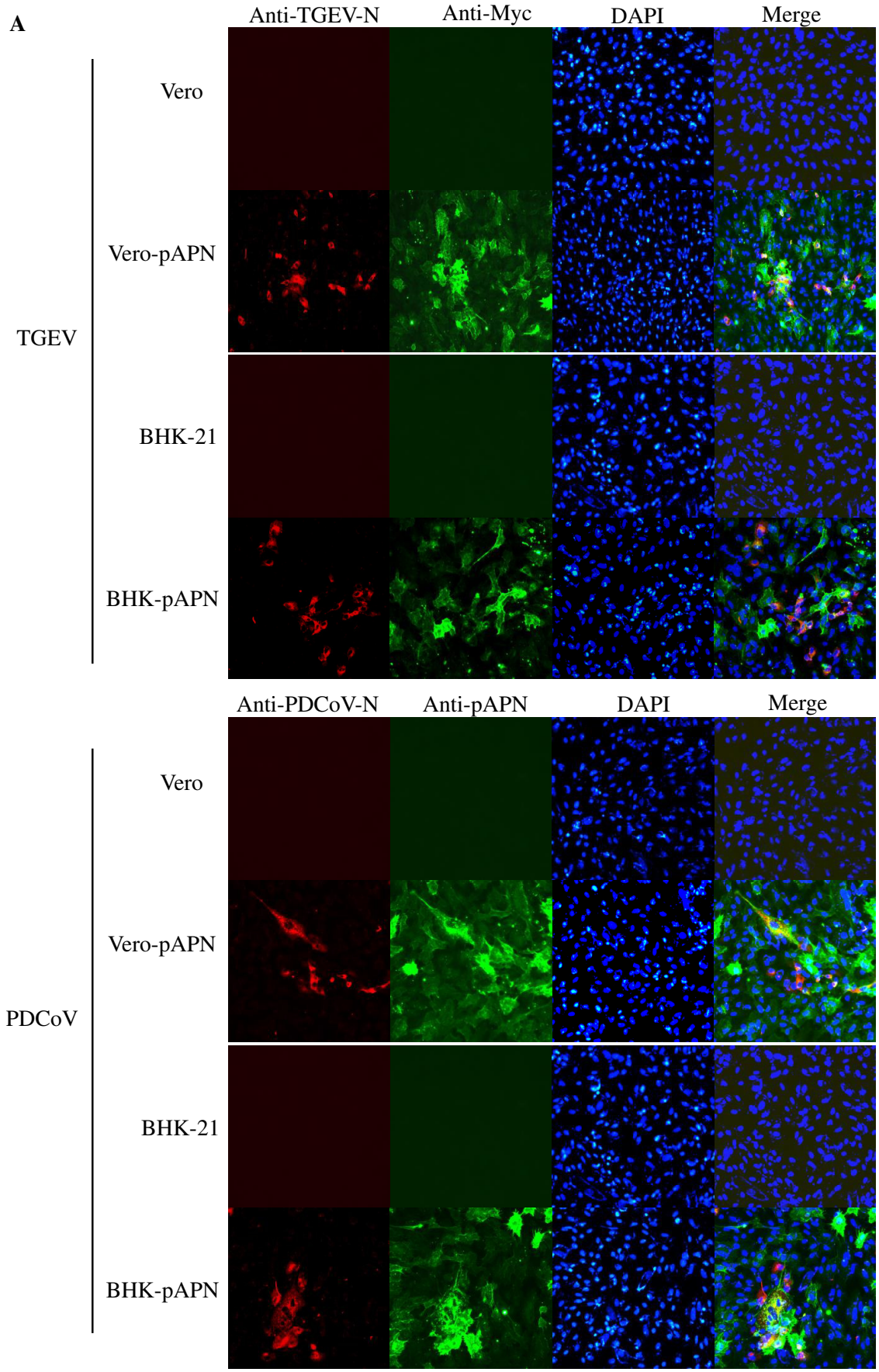

Fig. 4A

Fig. 4B

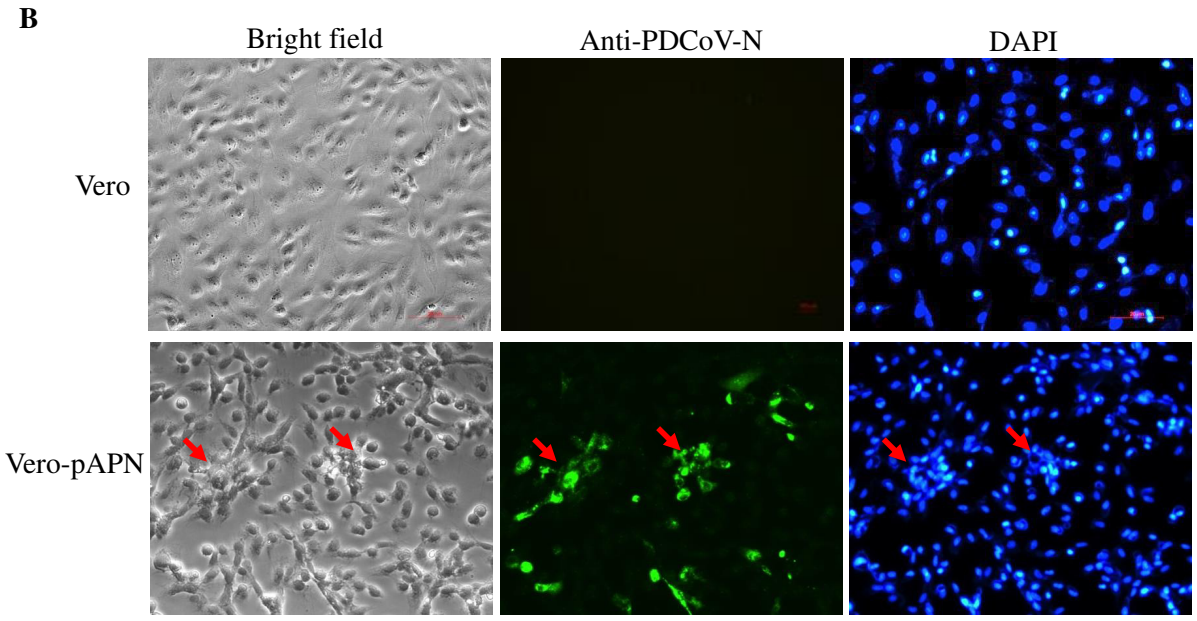

Fig. 5

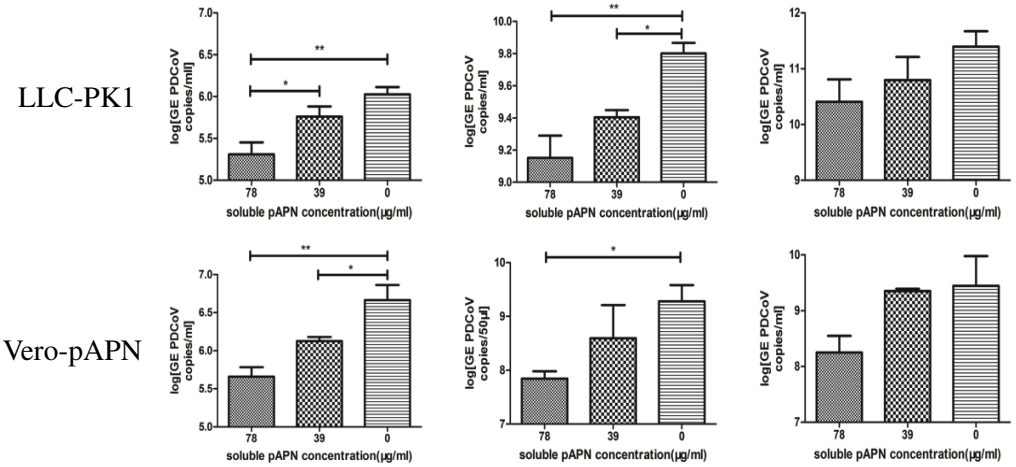

Fig. 6